Optics Letters

Extinction by a homogeneous spherical particle in an absorbing medium

Michael I. Mishchenko,[1,*] Gorden Videen,[2] and Ping Yang[3]

[1]NASA Goddard Institute for Space Studies, 2880 Broadway, New York, New York 10025, USA
[2]U.S. Army Research Laboratory, AMSRL-IS-EE, 2800 Powder Mill Road, Adelphi, Maryland 20783-1197, USA
[3]Department of Atmospheric Sciences, Texas A&M University, College Station, Texas 77843, USA
*Corresponding author: michael.i.mishchenko@nasa.gov

Received 29 September 2017; accepted 20 October 2017; posted 30 October 2017 (Doc. ID 308269); published 22 November 2017

We use a recent computer implementation of the first-principles theory of electromagnetic scattering to compute far-field extinction by a spherical particle embedded in an absorbing unbounded host. Our results show that the suppressing effect of increasing absorption inside the host medium on the ripple structure of the extinction efficiency factor as a function of the size parameter is similar to the well-known effect of increasing absorption inside a particle embedded in a nonabsorbing host. However, the accompanying effects on the interference structure of the extinction efficiency curves are diametrically opposite. As a result, sufficiently large absorption inside the host medium can cause negative particulate extinction. We offer a simple physical explanation of the phenomenon of negative extinction consistent with the interpretation of the interference structure as being the result of interference of the field transmitted by the particle and the diffracted field due to an incomplete wavefront resulting from the blockage of the incident plane wave by the particle's geometrical projection. © 2017 Optical Society of America

OCIS codes: (290.5850) Scattering, particles; (290.5825) Scattering theory; (290.2200) Extinction; (260.5740) Resonance.

https://doi.org/10.1364/OL.42.004873

The basic theory of frequency-domain electromagnetic scattering by a homogeneous spherical particle embedded in an absorbing unbounded host was formulated by Stratton [1] in 1941. Yet practical applications of this theory have been plagued by the long-lasting controversy caused by the poorly justified desire to preserve all the components of the conventional far-field Lorenz–Mie theory derived for the case of a nonabsorbing host medium [2–4], including all three optical cross sections (see, e.g., Ref. [5] and references therein). It is imperative to realize, however, that the introduction of an optical observable is only meaningful if it helps to (1) model theoretically the reading of a specific detector of electromagnetic radiation, and/or (2) quantify the electromagnetic energy budget of a finite volume of space [6]. Then in the context of the far-field formalism (including the radiative transfer theory) [6], in combination with the use of specific detectors of electromagnetic radiation called well-collimated radiometers (WCRs) [6], only two single-scattering characteristics remain meaningful. They are the (ensemble-averaged) extinction cross section and Stokes phase matrix [7–11].

The recent development of a numerically exact far-field Lorenz–Mie computer program [12] incorporating the absorbing-host scenario [9] makes possible a systematic quantitative study of both single-scattering characteristics. In this Letter, we focus on the extinction cross section of an isolated spherical particle and analyze its dependence on the particle size parameter $x = 2\pi R/\lambda$ and the complex refractive indices of the particle, $m_2 = m_2' + im_2''$, and the host medium, $m_1 = m_1' + im_1''$, where R is the particle radius, λ is the vacuum wavelength, and $i = (-1)^{1/2}$.

Let $k_1 = k_1' + ik_1'' = 2\pi m_1/\lambda$ be the complex wave number in the unbounded host medium. The extinction cross section C_{ext} appears in the context of quantifying the measurement with a WCR provided so that the instrument is located in the far zone of a particle, is centered at the particle, and has its optical axis along the propagation direction $\hat{\mathbf{n}}^{\text{inc}}$ of the incident plane electromagnetic wave (Fig. 1) [6]. Specifically, at a sufficiently large distance r from the particle, the reading of the WCR is given by

$$\text{WCR signal} \propto \exp(-2k_1''r)(S - C_{\text{ext}})I^{\text{inc}}, \tag{1}$$

where S is the area of the objective lens of the WCR, and I^{inc} is the intensity of the incident homogeneous (uniform) plane wave at the center of the particle. The extinction cross section is expressed in terms of the forward-scattering 2×2 amplitude matrix $\mathbf{S}(0)$ as follows [9]:

$$C_{\text{ext}} = \frac{2\pi}{k_1'}\text{Im}[S_{11}(0) + S_{22}(0)] = \frac{4\pi}{k_1'}\text{Im}S_{11}(0). \tag{2}$$

Thus, it is clear that the measurement of the extinction cross section is a two-step process wherein one records the reading of the WCR first in the presence of the particle and then in its absence. Importantly, the extinction cross section is independent of the distance from the particle and, thus, characterizes the particle itself [7–9]. According to Mishchenko and Yang [12], the specific expression for C_{ext} in the framework of the Lorenz–Mie theory is

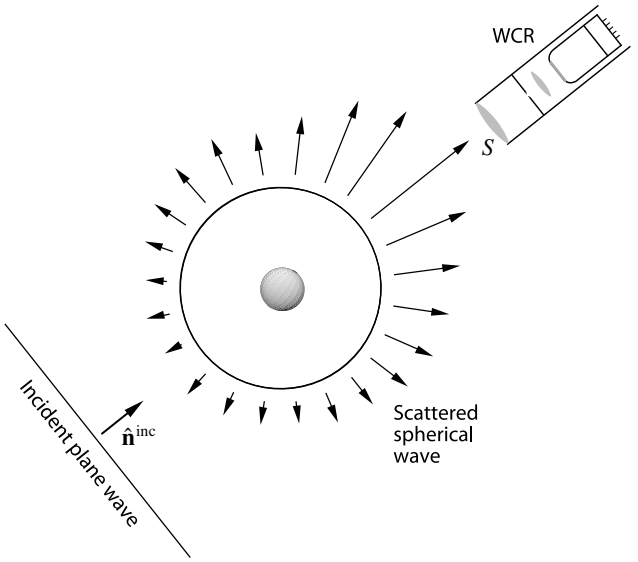

Fig. 1. Physical meaning of the extinction cross section.

$$C_{\text{ext}} = \frac{2\pi}{k_1'} \text{Re} \sum_{n=1}^{\infty} \frac{1}{k_1} (2n+1)(a_n + b_n), \tag{3}$$

where a_n and b_n are the Lorenz–Mie coefficients. This formula corrects Eq. (11) of Ref. [7]. Importantly, the distance-independent extinction cross section cannot be introduced in the context of evaluating the energy budget of an arbitrarily shaped volume containing the scattering particle [7–9,12].

We follow the conventional practice of normalizing the extinction cross section by the area of the particle geometrical projection and, thereby, plotting the dimensionless extinction efficiency factor $Q_{\text{ext}} = C_{\text{ext}}/(\pi R^2)$. Figure 2 shows Q_{ext} as a function of the size parameter for $m_2 = 1.4$, $m_1' = 1$, and $m_1'' = 0, 0.001, 0.02$, and 0.04. To make this specific plot, the extinction efficiency factor was computed at $\Delta x = 0.01$ intervals.

In the case of a nonabsorbing host medium with $m_1'' = 0$, the Q_{ext} curve is a succession of major low-frequency maxima and minima burdened by high-frequency ripples composed of (much) narrower quasi-irregularly spaced extrema, some of which are quite sharp. With an increase in the size parameter, the Q_{ext} values tend to the value 2, thereby illustrating the famous extinction paradox (see, e.g., Refs. [13,14] and references therein).

The succession of the pronounced maxima and minima is called the interference structure and is sometimes explained qualitatively as being the result of interference of the light transmitted by the particle and that diffracted by its geometrical projection in the near-forward direction [2,15,16]. Indeed, the portion of the incident plane wave passing through the center of the spherical particle accumulates a phase shift $\rho = 2x(m_2 - 1)$. As a consequence, constructive and destructive interference and the resulting maxima and minima in the bottom Q_{ext} curve occur at intervals $\approx 2\pi$ in ρ. An alternative qualitative explanation could be the interference of the incident plane wave with the surface plasmon. Indeed, at the first resonance, the phase difference between the incident wave and surface plasmon should be defined by $\lambda = \pi R - 2R$ (the difference in path lengths going straight through and along half the surface), or $x = 2\pi/(\pi - 2) \sim 5.5$, which is quite close to where the first peak is in Fig. 2. This explanation appears to be consistent with the persistence of the first interference maximum, even for strongly absorbing particles, i.e., when there is virtually no internal field (see Fig. 9.7 in Ref. [4]).

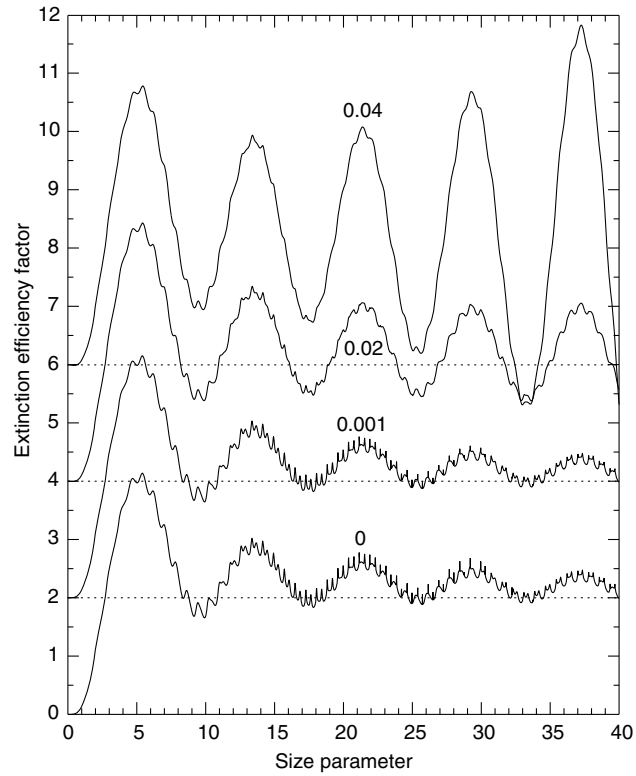

Fig. 2. Extinction efficiency factor versus the size parameter for $m_1' = 1$ and $m_2 = 1.4$. The four extinction curves are labeled by the value of m_1''. The vertical scale applies to the curve for $m_1'' = 0$, the other curves being successively displaced upward by 2.

Unlike the interference structure, the ripple is attributed to the erratic behavior of individual Lorenz–Mie coefficients (see, e.g., Refs. [17,18] and references therein). The resonances caused by lower-order coefficients are relatively broad and often overlap. However, as n increases, the resonance features become narrower so that, starting with $n \sim 20$, each so-called morphology-dependent resonance (MDR) (or "whispering-gallery mode") in the bottom curve can be attributed to an individual resonance in the corresponding Lorenz–Mie coefficient a_n or b_n.

The solid curves in Fig. 3 demonstrate that some of the MDRs can be extremely narrow and that the $\Delta x = 0.01$ resolution of Fig. 2 is grossly insufficient to accurately profile this specific resonance. Note that the bottom panel depicts the asymmetry parameter $\langle \cos \Theta \rangle$ defined as one-third of the first coefficient in the Legendre polynomial expansion of the phase function [12].

Figure 3 also reveals the evolution of the MDR centered at $x \approx 31.4738$ with growing m_1''. Obviously, raising m_1'' from zero to as small a value as 0.001 essentially annihilates this spike-like feature while causing almost no change in the background Q_{ext} and $\langle \cos \Theta \rangle$ values. Figure 2 reveals that it takes significantly greater m_1''-values to extinguish the broader resonances. In this respect, the effect of increasing m_1'' in the case of

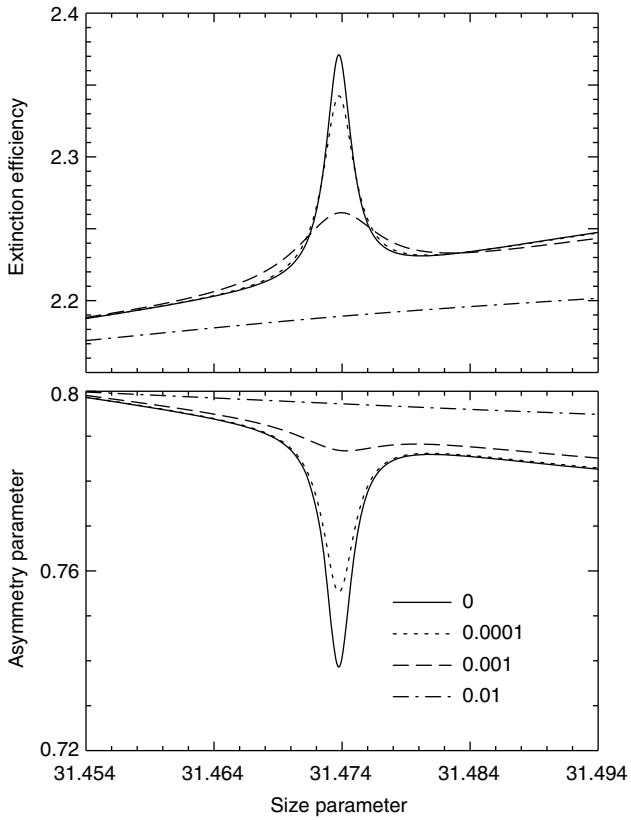

Fig. 3. Q_{ext} and $\langle \cos \Theta \rangle$ versus the size parameter for $m_1' = 1$ and $m_2 = 1.4$. The four curves are labeled by the value of m_1''.

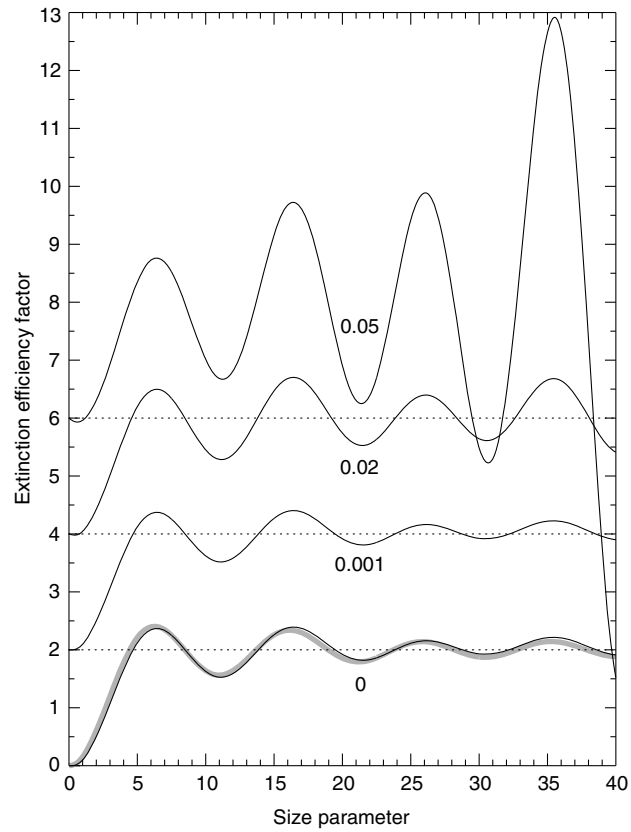

Fig. 4. Thin black curves, as in Fig. 1, but for $m_1' = 1.33$ and $m_2 = 1$. The thick gray curve is explained in the main text.

a real-valued m_2 is similar to that of increasing m_2'' in the case of a nonabsorbing host (see, e.g., Refs. [4,19,20] and references therein).

However, the corresponding effects on the interference structure are diametrically opposite. Indeed, in the case of a nonabsorbing host medium, the effect of increasing m_2'' is to progressively reduce the amplitude of the interference oscillations and ultimately make the extinction curve quite smooth and quite close to the canonical value 2 (see, e.g., Fig. 9.7 in Ref. [4]). In Fig. 2, however, the effect of increasing m_1'' is to "swing" the interference oscillations to the extent that for $m_1'' = 0.04$ and size parameters greater than about 32.4, the extinction efficiency factor can become *negative*. A by-product of this remarkable effect (which is fundamentally different from negative extinction typical of active particles [21–24]) could be to make questionable the general relevance of the extinction paradox.

Figure 4 pertains to the case of a spherical void (air bubble) in a $m_1' = 1.33$ material (such as water or water ice). Interestingly, the $m_1'' = 0$ curve exhibits no MDRs. This finding appears to be consistent with a qualitative interpretation of resonances as a scenario, wherein "light rays" propagate around the inside surface of a spherical particle while being confined by an almost total internal reflection [18]. Specifically, the rays approach the internal surface at an angle beyond the critical angle and are totally reflected each time. After having propagated around the sphere of just the right radius, a ray returns to its entrance point exactly in phase and then follows the same path again, without being attenuated by destructive interference. Since total internal reflection is impossible if $m_2/m_1 < 1$ (as is the case with the bottom thin black curve in Fig. 4), the ripple structure is also absent.

Figure 4 reveals that increasing m_1'' from 0 to 0.05 does not contribute any quasi-irregular high-frequency features similar to MDRs. However, it does amplify the low-frequency interference oscillations in the same way as in Fig. 2, once more to the point that the extinction efficiency factor becomes negative, as illustrated by the $m_1'' = 0.05$ curve. Again, this trait is opposite the effect of increasing absorption inside a spherical particle embedded in a nonabsorbing medium.

In summary, Figs. 2–4 represent numerically exact results based on the fundamental theory of far-field electromagnetic scattering by a spherical particle embedded in an absorbing unbounded host [9,12]. They show that the effect of increasing absorption inside the host medium on the ripple structure of the extinction efficiency curves is similar to the well-known effect of increasing absorption inside a particle embedded in a nonabsorbing host. However, the respective effects on the interference structure of Q_{ext} as a function of the size parameter are quite different. The resulting phenomenon of Q_{ext} becoming negative for sufficiently large values of m_1'' and x is obviously intriguing. Therefore, it is imperative to analyze whether this phenomenon is real or is an artifact of pushing Eqs. (1)–(3) beyond the limits of their applicability.

First, it is important to note that we have paid special attention to ensuring that our computer calculations of the Lorenz–Mie coefficients are numerically exact. To this end, we compared the results of running the computer program

developed by Mishchenko and Yang [12] with those based on a completely independent computer program described by Yang *et al.* [25] and based on a different set of recurrence relations for the special functions involved. The agreement between these two sets of results was essentially perfect, thereby confirming that negative C_{ext} values cannot be attributed to a flaw in the computer calculation of the right-hand side of Eq. (3).

Secondly, the very concept of extinction being the difference between two readings of a WCR in the absence and in the presence of the particle implies that negative C_{ext} values are not necessarily unphysical. Indeed, it is natural to expect that embedding a sufficiently large nonabsorbing particle in a strongly absorbing medium can serve to increase, rather than decrease the signal recorded by the WCR in Fig. 1, thereby making C_{ext} negative. On the other hand, the derivation of Eqs. (1) and (2) is inherently based on mathematically equivalent techniques such as the method of stationary phase, Jones' lemma [26], or the Saxon decomposition of a plane electromagnetic wave into incoming and outgoing spherical waves [27]. In the case of an absorbing host medium, the use of any of these approaches is based on the implicit assumption that

$$m_1'' \ll m_1'. \tag{4}$$

Therefore, it is not inconceivable that the values $m_1'' = 0.04$ in Fig. 2 and $m_1'' = 0.05$ in Fig. 4 are large enough to be inconsistent with the inequality (4). Furthermore, such m_1'' values are likely to make the exponential attenuation term in Eq. (1) very small at a far-field observation point, thereby making the practical applicability of the very concept of far-field particulate scattering potentially questionable.

On the other hand, it can be demonstrated that the behavior of the interference structure with increasing m_1'' in Figs. 2 and 4 is consistent with its qualitative explanation as being the result of interference of the light diffracted and transmitted by the particle. Indeed, let us assume that if there were no differential attenuation between the transmitted and diffracted fields, then the interference structure of Q_{ext} would largely be the same as that exhibited by the $m_1'' = 0$ curves in Figs. 2 and 4. However, if the host medium is absorbing and $m_2'' = 0$ (as is the case with Figs. 2 and 4), then unlike the field diffracted on the particle projection, the transmitted field is not subject to the $\exp(-2k_1''R)$ attenuation over the path length given by the particle diameter. This leads to an exponentially growing amplitude of the interference oscillations with increasing R in the case of nonzero m_1''. This explanation is illustrated by the thick gray curve in Fig. 4 showing the result of replacing Q_{ext} computed for $m_1'' = 0.05$ by $(Q_{\text{ext}} - 2)\exp(-2k_1''R) + 2$. It is seen indeed that the gray curve is virtually indistinguishable from the thin black curve corresponding to $m_1'' = 0$. This, in the final analysis, serves to confirm the physical relevance of the negative extinction phenomenon, as well as of the extinction paradox. According to Lock (personal communication), our explanation of negative extinction should be verifiable by a Debye series analysis of the partial wave scattering amplitudes [16].

Funding. National Aeronautics and Space Administration (NASA).

Acknowledgment. The authors thank Petr Chýlek, Zhanna Dlugach, Steven Hill, and James Lock for useful discussions, two anonymous reviewers for constructive suggestions, and Nadia Zakharova for help with graphics.

REFERENCES

1. J. A. Stratton, *Electromagnetic Theory* (McGraw Hill, 1941).
2. H. C. van de Hulst, *Light Scattering by Small Particles* (Wiley, 1957).
3. C. F. Bohren and D. R. Huffman, *Absorption and Scattering of Light by Small Particles* (Wiley, 1983).
4. M. I. Mishchenko, L. D. Travis, and A. A. Lacis, *Scattering, Absorption, and Emission of Light by Small Particles* (Cambridge University, 2002).
5. J. Yin and L. Pilon, J. Opt. Soc. Am. A **23**, 2784 (2006).
6. M. I. Mishchenko, *Electromagnetic Scattering by Particles and Particle Groups: An Introduction* (Cambridge University, 2014).
7. C. F. Bohren and D. P. Gilra, J. Colloid Interface Sci. **72**, 215 (1979).
8. G. Videen and W. Sun, Appl. Opt. **42**, 6724 (2003).
9. M. I. Mishchenko, Opt. Express **15**, 13188 (2007).
10. M. I. Mishchenko, Opt. Express **16**, 2288 (2008).
11. M. I. Mishchenko, J. Quant. Spectrosc. Radiat. Transfer **109**, 2386 (2008).
12. M. I. Mishchenko and P. Yang, J. Quant. Spectrosc. Radiat. Transfer **205**, 241 (2018).
13. L. Brillouin, J. Appl. Phys. **20**, 1110 (1949).
14. M. J. Berg, C. M. Sorensen, and A. Chakrabarti, J. Quant. Spectrosc. Radiat. Transfer **112**, 1170 (2011).
15. P. Chýlek and J. Zhan, J. Opt. Soc. Am. A **6**, 1846 (1989).
16. J. A. Lock and L. Yang, J. Opt. Soc. Am. A **8**, 1132 (1991).
17. P. Chýlek, J. Opt. Soc. Am. **66**, 285 (1976).
18. S. C. Hill and R. E. Benner, *Optical Effects Associated with Small Particles*, P. W. Barber and R. K. Chang, eds. (World Scientific, 1988), p. 3.
19. G. Videen and W. S. Bickel, Phys. Rev. A **45**, 6008 (1992).
20. G. Videen and P. Chýlek, J. Opt. Soc. Am. A **12**, 916 (1995).
21. N. G. Alexopoulos and N. K. Uzunoglu, Appl. Opt. **17**, 235 (1978).
22. M. Kerker, Appl. Opt. **17**, 3337 (1978).
23. M. Kerker, Appl. Opt. **18**, 1180 (1979).
24. M. Kerker, D.-S. Wang, H. Chew, and D. D. Cooke, Appl. Opt. **19**, 1231 (1980).
25. P. Yang, B.-C. Gao, W. J. Wiscombe, M. I. Mishchenko, S. E. Platnick, H.-L. Huang, B. A. Baum, Y. X. Hu, D. M. Winker, S.-C. Tsay, and S. K. Park, Appl. Opt. **41**, 2740 (2002).
26. D. S. Jones, Proc. Cambridge Philos. Soc. **48**, 733 (1952).
27. D. S. Saxon, Phys. Rev. **100**, 1771 (1955).